Optimal Utilization of Microgrids Supplemented with Battery Energy Storage Systems in Grid Support Applications

Anvari-Moghaddam, Amjad; Dragicevic, Tomislav; Vasquez, Juan Carlos; Guerrero, Josep M.

Published in:
Proceedings of the 2015 IEEE First International Conference on DC Microgrids (ICDCM)

DOI (link to publication from Publisher):
10.1109/ICDCM.2015.7152010

Publication date:
2015

Document Version
Early version, also known as pre-print

Citation for published version (APA):
Anvari-Moghaddam, A., Dragicevic, T., Vasquez, J. C., & Guerrero, J. M. (2015). Optimal Utilization of Microgrids Supplemented with Battery Energy Storage Systems in Grid Support Applications. In *Proceedings of the 2015 IEEE First International Conference on DC Microgrids (ICDCM)* (pp. 57 - 61). IEEE Press. https://doi.org/10.1109/ICDCM.2015.7152010

Optimal Utilization of Microgrids Supplemented with Battery Energy Storage Systems in Grid Support Applications

Amjad Anvari-Moghaddam, Tomislav Dragicevic, Juan C. Vasquez and Josep M. Guerrero
Department of Energy Technology,
Aalborg University,
Aalborg, Denmark, tdr@et.aau.dk
Email: {aam,tdr,juq,joz}@et.aau.dk

***Abstract*—This paper proposes a control scheme which minimizes the operating cost of a grid connected micro-grid supplemented by battery energy storage system (BESS). What distinguishes approach presented here from conventional strategies is that not only the price of electricity is considered in the formulation of the total operating cost but an additional item that takes into account inevitable battery degradation. The speed of degradation depends on battery technology and its mission profile and this effect demands for eventual replacement of the stack. Therefore it can be mapped in additional operating cost. By modeling battery degradation as a function of depth of discharge (DoD) and discharge rate and translating incremental loss of capacity in each cycle into associated cost, objective function has been defined and solved using GAMS. Simulation results are presented to verify the proposed approach.**

Keywords—Energy management; battery energy storage system; DC micro-grid; economic dispatch.

I. INTRODUCTION

With technological improvements in battery energy storage systems (BESSs) and proliferation of renewable energy sources (RESs) such as photovoltaic (PVs) panels and wind turbines (WTs), concept of micro-grid (MG) began to be conceived as a kind of energy hub which can efficiently aggregate these units and show itself as a unitary whole [1]-[2]. Typical MG can operate either in grid connected or autonomous mode [3]-[4]. From the storage point of view, its role in autonomous mode is simply to compensate the imbalance of power between intermittent RES and loads [5]-[6]. On the other hand, grid connected mode allows much more flexibility in optimizing its real time operation since it can be interactively decided whether to utilize energy from the grid of storage [5]. In this work, we present the complete mathematical formulation of the problem in which a scenario of grid-connected MG supplemented with BES is considered and the customers that are supplied from it are interested to minimize their electricity bill. This kind of a MG may present a local household or commercial facility that aims to create savings by taking advantage of variable electricity price policy which is implemented in many developed countries around the world [7]-[9]. The optimization problem presented in next section is solved in centralized fashion. One option is to apply this optimal strategy to tertiary layer of a classical MG hierarchical control system and interface to lower layers via low bandwidth digital communication technology [10]. Another option is to analyze the optimal results and map them into local decentralized control that would result in near-optimal solution but with reduced implementation cost. One example of such an approach is presented in [11].

II. SYSTEM DESCRIPTION

Block diagram of a DC micro-grid that is operated in grid-connected mode is shown in Fig. 1. It is comprised of RESs such as PV panels, WTs, battery ESS and grid connection.

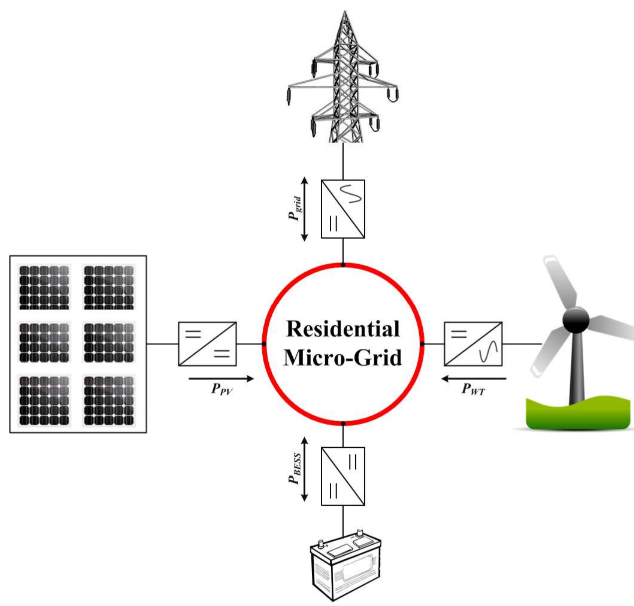

Fig. 1. Schematic layout of a generic DC microgrid.

Power flows between the MG and each of the respective components is regulated via power electronics interface. RESs are operated in Maximum Power Point Tracking (MPPT) mode and loads are considered to be uncontrollable. In this sense, powers exploited from the grid and from the battery ESS present the only two degrees of freedom for fulfilling the load balance. It should be noted that battery SOC also presents a limitation since battery cannot be freely used in extreme cases when the SOC is very high or very low. Still, this limitation is much more apparent in stand-alone mode since it then provides additional degrees of freedom in control. More precisely, possibility of using the grid for obtaining the load balance is exchanged on one hand by controllable RES which are demanded to reduce their power production when SOC is too high. On the other hand, load shedding is commonly used when SOC is too low [12].

In this paper, higher level control of a grid-connected DC MG with aforementioned architecture is proposed. For that matter, issues such as primary voltage and current control, as well as stability are not taken into account and system is assumed to be well tuned. Incorporation of strategy developed here into a complete solution that considers both local and coordinated control functionalities is a subject of present investigation. Complete mathematical formulation of the problem is presented next.

III. Problem Formulation

In this work, optimal operation of a renewable grid-connected MG supplemented with BESS, is formulated as an optimization problem considering minimization of the total operation cost as the objective and different system's technical aspects as constraints. The total cost of operation in short-term includes the costs of power exchange with the utility and the battery degradation cost:

$$Min:\ Cost = \sum_{k=1}^{T}\left(\rho_{grid}(k)\cdot P_{grid}(k) + \rho_{Batt}(k)\cdot P_{Batt,dch}(k)\right) \quad (1)$$

where, $\rho_{grid}(k)$ and $P_{grid}(k)$are the real-time electricity price and the amount of power bought (or sold) from (or to) the utility at time k, respectively. Likewise, $\rho_{Batt}(k)$ is the marginal cost of battery in DKK/kWh that indicates the incremental costs induced for additional electricity generation of 1 kWh and represents the degradation cost of BESS.

To keep high battery efficiency, the charging/discharging power and the State of Charge (SOC) should be constrained within certain ranges as follows:

$$P_{Batt,ch}(k) \le P_{ch,\max}\cdot\eta_{ch}\cdot u_{Batt}(k) \quad (2)$$

$$P_{Batt,dch}(k) \le \left(\frac{P_{dch,\max}}{\eta_{dch}}\right)\cdot\left(1-u_{Batt}(k)\right) \quad (3)$$

$$SOC_{\min} \le SOC(k) \le SOC_{\max} \quad (4)$$

where, $P_{ch,max}$ and $P_{dch,max}$ are the battery maximum charging and discharging powers and SOC_{min} and SOC_{max} are the lower and upper bounds of the battery's SOC, respectively. In a similar manner, η_{ch} and η_{dch} are the battery's charging and discharging efficiencies, and $u_{Batt}(k)$ is a binary variable that shows the battery's status at iteration k ("1"=charging and "0"=discharging). Considering the above constraints, the SOC update function is given by:

$$SOC(k+1) = SOC(k) + \frac{\left(P_{Batt,ch}(k) - P_{Batt,dch}(k)\right)\delta_t}{E_{Batt}} \quad (5)$$

where, E_{Batt} is the battery capacity in kWh and δ_t is the iteration cycle duration. It should be mentioned that each battery cell has a finite life as measured by the sum of the effective ampere-hours (*Ah*) throughput during its useful life[13]-[14]. Generally, this life is affected by the depth of discharge (DoD) and the discharging rate of BESS as described below[15].

A. Effect of depth of discharge on cell charge life

When the cumulative effective ampere-hours (*EAh*), expressed as the sum of the individual *EAh*s corresponding to a number of discharge events, equals the rated charge life (Γ_R) of a battery cell, the cell will reach its useful life. The rated charge life of the cell is defined as:

$$\Gamma_R = L_R D_R C_R \quad (6)$$

in which, L_R refers to the rated life cycle, D_R is the DoD for which the rated cycle life is determined, and C_R is the rated *Ah* capacity at rated discharging current I_R. Similarly, the actual charge life of a battery cell is a function of the DoD at which it is cycled; i.e., depending on the actual DoD with respect to the rated DoD, the *EAh* discharge in a given discharge event may be more or less than the actual discharge. In this regard, (7) could be used to evaluate the influence of depth of discharge on cycle life[16]:

$$L = u_2\left(\frac{D_R}{D}\right)^{u_o} e^{u_1\left(1-\frac{D}{D_R}\right)} \quad (7)$$

where D denotes the absolute discharge relative to the rated cell capacity and u_0, u_1 and u_2 are the coefficients determined based on curve fitting for experimental test as shown in Fig. 2.

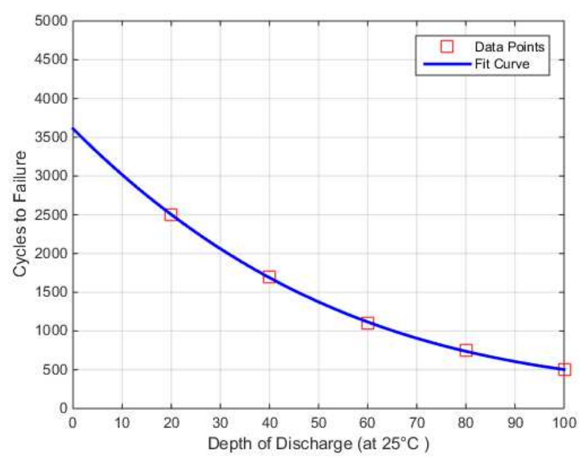

Fig. 2. Typical life data and fit curve for pocket plate NiCd cells [17]

Having found the aforementioned coefficients, the effective discharge (*EAh*) for a given discharge event can be expressed by making the substitutions $L_R = u_2$, $d_{eff}/d_A = L_R/\mathrm{L}$ and rearranging (7) as follow:

$$d_{eff} = d_A \left(\frac{D_A}{D_R}\right)^{u_0} e^{u_1\left(\frac{D_A}{D_R}-1\right)} \tag{8}$$

where d_{eff} and d_A are the effective and actual discharge, respectively.

B. Effect of discharge rate

Similar to the influence of DoD, the discharge rate of the battery also affects the battery's cycle life. The battery stresses more when higher currents are demanded from it and the increased stress will likely ends in shorter battery life. The effect of discharge rate on the effective discharge for a given discharge event can be expressed based on the following simplified expression:

$$d_{eff} = d_A \left(\frac{C_R}{C_A}\right)^{v_0} e^{v_1\left(\frac{C_R}{C_A}-1\right)} \tag{9}$$

in which C_A is the actual capacity at actual discharging current obtained from the "amperes-on-discharge" datasheet provided by the battery manufacturer and coefficients v_0 and v_1 are determined based on curve fitting for experimental test as shown in Fig. 3.

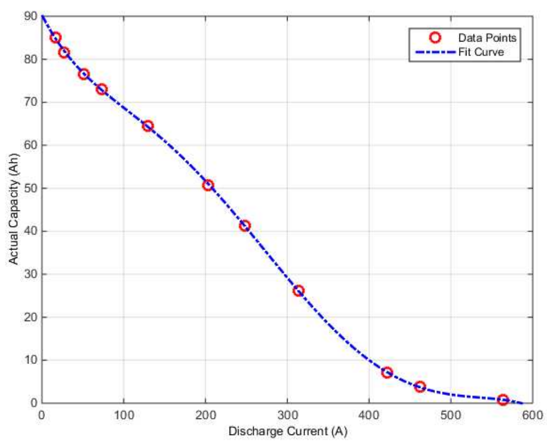

Fig. 3. Actual capacity versus discharge current for 85 Ah NiCd Cell [14]

The effects of DOD and discharge rate are combined simply by multiplying the factors expressed in (8), (9):

$$d_{eff} = d_A \left(\frac{D_A}{D_R}\right)^{u_0} e^{u_1\left(\frac{D_A}{D_R}-1\right)} \left(\frac{C_R}{C_A}\right)^{v_0} e^{v_1\left(\frac{C_R}{C_A}-1\right)} \tag{10}$$

If it is assumed that the output of battery remains fixed in every iteration cycle, the actual discharge of battery in iteration k is:

$$d_A(k) = \frac{P_{Batt,dch}(k)}{v(k)}\delta_t \tag{11}$$

where $v(k)$ is the battery terminal voltage at the k^{th} iteration. Likewise, BESS cost ($Cost_{BESS}(k)$) during iteration k can be calculated as follows:

$$\begin{aligned} Cost_{BESS}(k) &= \left(\frac{RC}{\Gamma_R}\right) d_{eff}(k) \\ &= \left(\begin{aligned} &\delta_t \times \left(\frac{RC}{\Gamma_R}\right) \times \left(\frac{P_{Batt,dch}(k)}{v(k)}\right) \times \left(\frac{C_R}{C_A(k)}\right)^{v_0} \\ &\times \left(\frac{D_A(k)}{D_R}\right)^{u_0} \times e^{u_1\left(\frac{D_A(k)}{D_R}-1\right)} \times e^{v_1\left(\frac{C_R}{C_A(k)}-1\right)} \end{aligned} \right) \end{aligned} \tag{12}$$

where RC is the replacement cost of battery. In a similar manner, the marginal cost of battery in DKK/kWh can be also expressed as:

$$\rho_{Batt}(k) = \left(\begin{aligned} &\left(\frac{RC}{\Gamma_R v(k)}\right) \times \left(\frac{C_R}{C_A(k)}\right)^{v_0} \times \left(\frac{D_A(k)}{D_R}\right)^{u_0} \\ &\times e^{u_1\left(\frac{D_A(k)}{D_R}-1\right)} \times e^{v_1\left(\frac{C_R}{C_A(k)}-1\right)} \end{aligned} \right) \tag{13}$$

It is worthy of note that the proposed objective function must be optimized subject to the following demand-supply balance and other technical constraints associated with the operation of distributed generation (DG) units and BESS.

$$P_{grid} + P_{PV} + P_{WT} - P_{Batt} = P_{Load} \tag{14}$$

IV. Computer Simulations

In this section, the simulation results are presented to show the performance of the proposed scheme in operation management of a typical DC micro-grid. In this regard, a residential MG with a given load profile, as shown in Fig. 4, is considered as the case study. In the same figure the real time utility electricity prices (RTP) are plotted for the examined period.

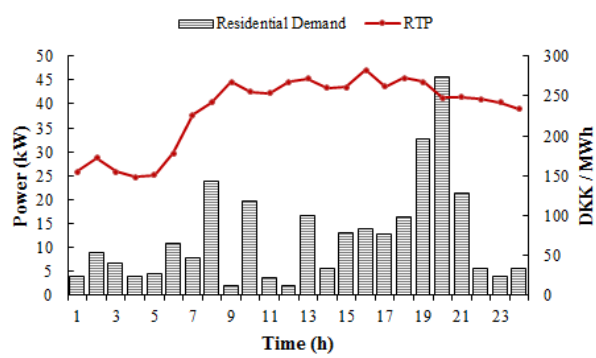

Fig. 4. Residential demand and RTP profiles

To simulate DGs in the analysis, a Morphic SWT20 type with 20 kW rated power at a wind speed of 9 m/s is used as a WT model in the proposed residential MG. The mentioned system is a direct driven, variable speed, pitch controlled WT whose related parameters are adopted from[18] . Likewise, Hyundai mono-crystalline solar module with a rated power of 0.25 kW is applied as the building block of the PV system[19]. In the computer simulation, the storage device is also modeled based on NiCd battery pack considering the specifications expressed in Table I. Other environmental conditions such as hourly temperature, wind speed and solar radiation at the studied place are tabulated in Table II.

It should be mentioned that all of the algorithms and simulations are carried out on a PC with an Intel i5-2430M chip running Windows 7(64 bit) with GAMS and Cplex/Dicopt solvers.

TABLE I. BESS SPECIFICATIONS [14]

Parameters	Value	Unit
Battery Pack Data		
$P_{Batt,ch}$, $P_{Batt,dch}$	33, 33	*kW*
SOC_{min},SOC_{max}	20 , 80	*%*
η_{ch}, η_{dch}	87, 90	*%*
Cell Information		
Nominal capacity (C_R)	85	*Ah*
Nominal charge life (Γ_R)	175000	*Ah*
Rated voltage	230	*V*

TABLE II. METEOROLOGICAL DATA [20]

Hour	Irradiation (W/m2)	Temp (oC)	Wind (m/s)	Hour	Irradiation (W/m2)	Temp (oC)	Wind (m/s)
1	0.0	13	4.12	**13**	857.2	18	3.09
2	0.0	12	2.57	**14**	836.2	18	2.57
3	0.0	10	1.54	**15**	772.9	19	3.09
4	0.0	10	0.51	**16**	672.3	19	3.60
5	34.4	10	0.00	**17**	543.1	18	3.09
6	115.4	12	0.51	**18**	396.8	19	4.12
7	242.7	12	0.51	**19**	248.9	17	4.63
8	390.1	13	1.03	**20**	120.3	15	4.63
9	536.9	16	2.06	**21**	36.8	14	3.60
10	667.2	17	1.54	**22**	0.0	12	2.57
11	769.2	17	2.06	**23**	0.0	12	4.12
12	834.3	18	2.57	**24**	0.0	12	2.57

The simulation results for the MG operation management and BESS optimal performance are shown in Fig. 5 and Fig. 6, respectively.

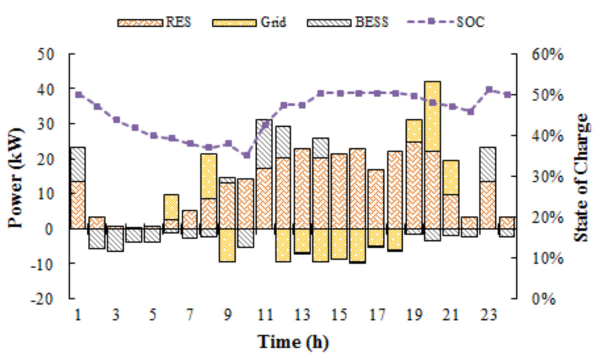

Fig. 5. Optimal operation of micro-gird

As it can be seen in Fig. 5, during some periods of time when the real-time electricity prices and the amount of power from renewable energy sources (RESs) are relatively low, most of the residential load is supplied by the utility; and the charging process of the battery is done with lower costs. With the growth of demand and bids of the utility during the other hours of the day, the BESS, not only generate electricity in a cost effective way to meet the load, but also sell the surplus of energy to the utility and make profits. Moreover, as observed from Fig. 6 with high penetration of renewables into the MG environment during the midday and in the afternoon, the discharge of BESS is stopped due to the degradation cost of batteries and the load is supplied by RESs.

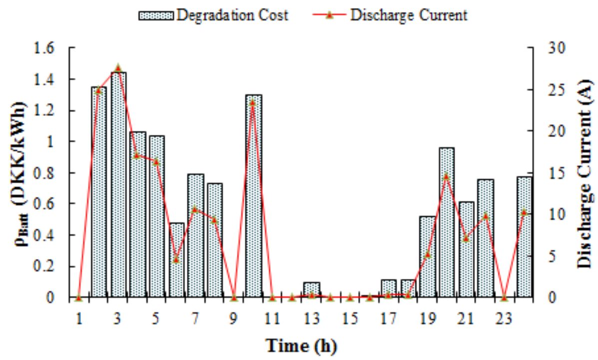

Fig. 6. Marginal costs of battery operation at discharge cycles

V. CONCLUSION

In this paper, an optimization scheme has been proposed for energy scheduling in a residential grid-connected micro-grid (MG) supplemented by battery energy storage system. The objective function has been defined as the minimization of total operation cost in short-term for the examined MG and includes the costs of power exchange with the utility and the battery degradation cost. While the cost of power exchange with the utility depends on the real-time electricity prices, battery degradation cost relies largely on battery usage pattern, discharge events (in terms of depths of discharge and discharge rate), cycle life and capacity data commonly available from battery manufacturers. It has been also demonstrated through computer simulations that the proposed optimization scheme could easily manage DG units in a way to reduce the cost of operation and meet available system constraints and objectives.

REFERENCES

[1] R. H. Lasseter, “MicroGrids,” in 2002 IEEE Power Engineering Society Winter Meeting. Conference Proceedings (Cat. No.02CH37309), vol. 1, pp. 305–308.

[2] N. Hatziargyriou, H. Asano, R. Iravani, and C. Marnay, “Microgrids,” Power Energy Mag., IEEE, vol. 5, no. 4, pp. 78–94, Jul. 2007.

[3] F. Katiraei, M. R. R. Iravani, and P. W. W. Lehn, “Micro-Grid Autonomous Operation During and Subsequent to Islanding Process,” IEEE Trans. Power Deliv., vol. 20, no. 1, pp. 248–257, Jan. 2005.

[4] J. A. Pecas Lopes, C. L. Moreira, and A. G. Madureira, “Defining control strategies for MicroGrids islanded operation,” IEEE Trans. Power Syst., vol. 21, no. 2, pp. 916–924, 2006.

[5] J. M. Guerrero, J. C. Vasquez, J. Matas, L. G. de Vicuna, and M. Castilla, “Hierarchical Control of Droop-Controlled AC and DC Microgrids—A General Approach Toward Standardization,” IEEE Trans. Ind. Electron., vol. 58, no. 1, pp. 158–172, Jan. 2011.

[6] T. Dragicevic, J. M. Guerrero, J. C. Vasquez, and D. Skrlec, “Supervisory Control of an Adaptive-Droop Regulated DC Microgrid With Battery Management Capability,” Power Electron. IEEE Trans., vol. 29, no. 2, pp. 695–706, 2014.

[7] H. Kakigano, Y. Miura, and T. Ise, “Configuration and control of a DC microgrid for residential houses,” in Transmission Distribution Conference Exposition: Asia and Pacific, pp. 1–4, 2009.

[8] B. T. Patterson, “DC, Come Home: DC Microgrids and the Birth of the ‘Enernet,’” Power Energy Mag. IEEE, vol. 10, no. 6, pp. 60–69, 2012.

[9] D. Boroyevich, I. Cvetkovic, D. Dong, R. Burgos, F. Wang, and F. Lee, “Future Electronic Power Distribution Systems: A Contemplative View,” in International Conference on Optimization of Electrical and Electronic Equipment, 2010, pp. 1369–1380.

[10] T. Dragicevic, Hierarchical Control of a Direct Current Microgrid with Energy Storage Systems in a Distributed Topology. PhD Thesis, 2013, p. 183.

[11] T. Dragicevic, J. Guerrero, and J. C. Vasquez, “A Distributed Control Strategy for Coordination of an Autonomous LVDC Microgrid Based on Power-Line Signalling,” IEEE Trans. Ind. Electron., vol. PP, no. 99, p. 1, 2013.

[12] D. Wu, F. Tang, T. Dragicevic, J. M. Guerrero, and J. C. Vasquez, “Coordinated Control Based on Bus-Signaling and Virtual Inertia for Islanded DC Microgrids,” IEEE Trans. Smart Grid, vol. PP, no. 99, p. 1, 2015.

[13] S. A. Pourmousavi, R. K. Sharma, and B. Asghari, "A framework for real-time power management of a grid-tied microgrid to extend battery lifetime and reduce cost of energy," in Innovative Smart Grid Technologies (ISGT), 2012 IEEE PES, pp. 1-8, 2012.

[14] S. Drouilhet and B. L. Johnson, "A Battery Life Prediction Method for Hybrid Power Applications," presented at the AIAA Aerospace Sciences Meeting and Exhibit, 1997.

[15] D. P. Jenkins, J. Fletcher, and D. Kane, "Lifetime prediction and sizing of lead-acid batteries for microgeneration storage applications," Renewable Power Generation, IET, vol. 2, pp. 191-200, 2008.

[16] R. Somogye “An Aging Model of Ni-MH Batteries for Use in Hybrid-Electric Vehicles”, Master Thesis, The Ohio State University, Columbus, 2004.

[17] Nickel–Cadmium Batteries, [Online]. Available: www.evdl.org/docs/ nicad-principles.pdf (2015, March 15).

[18] A. Anvari-Moghaddam, H. Monsef and A. Rahimi-Kian, “Cost-Effective and Comfort-Aware Residential Energy Management under Different Pricing Schemes and Weather Conditions”, Energy and Buildings, vol. 86, pp. 782-793, 2015.

[19] A. Anvari-Moghaddam, H. Monsef, and A. Rahimi-Kian, “Optimal Smart Home Energy Management Considering Energy Saving and a Comfortable Lifestyle”, IEEE Trans. on Smart Grid, vol.6, no.1, pp. 324-332, 2015.

[20] Weather Forecast for Denmark, [Online]. Available: http://www.dmi.dk /en /vejr (2014, June 23)